A LETTERS JOURNAL EXPLORING THE FRONTIERS OF PHYSICS

OFFPRINT

Measurement of the vortex core in sub-100 nm Fe dots using polarized neutron scattering

IGOR V. ROSHCHIN, CHANG-PENG LI, HARRY SUHL, XAVIER BATLLE, S. ROY, SUNIL K. SINHA, S. PARK, ROGER PYNN, M. R. FITZSIMMONS, JOSE MEJÍA-LÓPEZ, DORA ALTBIR, A. H. ROMERO and IVAN K. SCHULLER

EPL, **86** (2009) 67008

A Letters Journal Exploring the Frontiers of Physics

June 2009

EPL, **86** (2009) 67008
doi: 10.1209/0295-5075/86/67008

www.epljournal.org

Measurement of the vortex core in sub-100 nm Fe dots using polarized neutron scattering

Igor V. Roshchin[1,2], Chang-Peng Li[2(a)], Harry Suhl[2], Xavier Batlle[3], S. Roy[2(b)], Sunil K. Sinha[2], S. Park[4(c)], Roger Pynn[4(d)], M. R. Fitzsimmons[4], Jose Mejía-López[5], Dora Altbir[6], A. H. Romero[7] and Ivan K. Schuller[2]

[1] *Physics Department, Texas A&M University - College Station, TX, 77843-4242, USA*
[2] *Physics Department, University of California-San Diego - La Jolla, CA 92093-0319, USA*
[3] *Departament de Fisica Fonamental, Universitat de Barcelona - 08028 Barcelona, Catalonia, Spain, EU*
[4] *Los Alamos National Laboratory - Los Alamos, NM 87545, USA*
[5] *Facultad de Física, Pontificia Universidad Católica de Chile - Santiago, Chile*
[6] *Departamento de Física, Universidad de Santiago de Chile (USACH) - Santiago, Chile*
[7] *Materials Department, CINVESTAV - Querétaro, Mexico*

received 2 December 2008; accepted in final form 2 June 2009
published online 10 July 2009

PACS 75.75.+a – Magnetic properties of nanostructures
PACS 75.60.-d – Domain effects, magnetization curves, and hysteresis
PACS 61.05.F- – Neutron diffraction and scattering

Abstract – We use polarized neutron scattering to obtain quantitative information about the magnetic state of sub-100 nm circular magnetic dots. Evidence for the transition from a single domain to a vortex state, as a function of the dot diameter and magnetic field, is found from magnetization curves and confirmed by micromagnetic and Monte-Carlo simulations. For 20 nm-thick Fe dots with diameters close to 60 nm, the vortex is the ground state. The magnetization of the vortex core (140 ± 50 emu/cm^3) and its diameter (19 ± 4 nm) obtained from polarized neutron scattering are in agreement with simulations.

Introduction. – Magnetic vortices [1,2], a magnetization vector field with non-zero chirality, appearing in nano- and micrometer-sized elements have attracted much basic interest recently due to an ever increasing demand for high-density magnetic recording. In particular, magnetization reversal involving magnetic vortices has been studied in a wide variety of patterned structures [1–10]. Since the first imaging of magnetic vortices in permalloy (Py) sub-1 μm disks using magnetic force microscopy (MFM) [1], many efforts have focused on the 3D spin structure and magnetic reversal via the vortex state [3–5], vortex dynamics [6–8] and switching of the vortex core polarity [9,10], and vortex chirality [11], in dots, rings, and other micro- and nano-patterned structures. Those studies were performed by magneto-optical Kerr effect (MOKE) magnetometry, magnetic-resonance measurements, magnetization-sensitive microscopies, such as MFM, scanning electron or ion microscopy with polarization analysis (SEMPA and SIMPA, respectively), spin-polarized scanning tunneling microscopy (SP-STM), X-ray magnetic circular dichroism (XMCD), and Lorenz microscopy. Most experiments were performed with planar structures whose in-plane size was much larger than 100 nm. Imaging the vortex in sub-100 nm structures is limited by the resolution of the tools [3,8][1] and therefore is only qualitative without quantification of the magnetization or size of the vortex core. Particularly, scanning probe techniques provide a convolution of the tip structure with the magnetic structures of interest and therefore quantitative determination is hampered by the detailed knowledge of the tip structure [1,3]. For example, the vortex core sizes were measured with

[(a)] Present address: Physics Department, University of Michigan - Ann Arbor, MI, USA.
[(b)] Present address: Advanced Light Source, LBNL - Berkeley, CA, USA.
[(c)] Present addres: Physics Department, Pusan National University - Pusan, Korea.
[(d)] Present address: Physics Department, University of Indiana - Bloomington, IN, USA.

[1] So far we have been unable to reproducibly resolve the vortex core with SEMPA or MFM. We are aware of only two successful prior imagings of a vortex core [3,8].

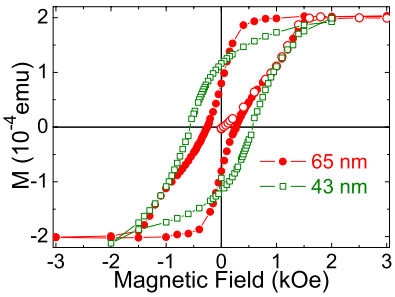

Fig. 1: (Colour on-line) Hysteresis loops for 43 nm (□) and 65 nm (●) diameter, 20 nm-thick Fe dots at 10 K (○ —virgin curve for 65 nm dots).

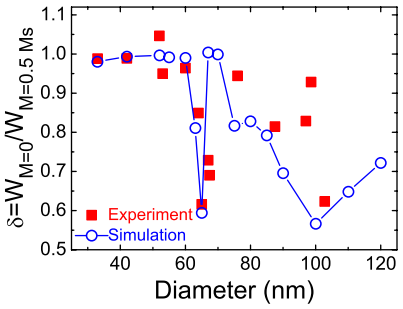

Fig. 2: (Colour on-line) δ as a function of the dot diameter obtained from measured magnetization curves (■) and MC simulation (○).

SIMPA [5] and XMCD [8] in sub-1 micron elements, and with SP-STM in 150–500 nm elements [3], although quantitative information about core magnetization was not obtained. This information is important *e.g.* for studies of core dynamics [6–10] and interaction with superconductors [12].

Here, we present a quantitative polarized neutron scattering measurement of the out-of-plane (OOP) magnetization of the vortex core in sub-100 nm Fe nanodots. Using SQUID magnetometry and micromagnetic (MM) and Monte Carlo (MC) simulations, we find the range of dot diameters for which the reversal of in-plane magnetization occurs via motion of a vortex, and the vortex is the ground state of the dots at remanence. Next, we establish the range of fields for which the vortex state is present in those dots. Using Grazing Incidence Small-Angle Neutron Scattering (polarized GI-SANS), we obtain the magnitude of the OOP magnetization and the corresponding vortex core size (independently of magnetometry) in good agreement with MM and MC simulations.

Samples and magnetization: measurements and simulations. – Hexagonally ordered polycrystalline Fe dots (20 nm thick) are prepared using anodized alumina masks on silicon substrates [13]. Dot diameters in the range 25–150 nm and periodicities, which are twice as large, have narrow distributions (10% standard deviation). The magnetic response of the array reflects the average response of a single dot because with the periodicity-diameter ratio of ~ 2, dipolar interactions between the dots can be neglected [14,15]. Porous alumina lithography provides macroscopic area samples, which enable the use of bulk magnetometry and neutron scattering, in contrast to most other lithographic techniques.

MC simulations are performed using the Metropolis algorithm with local dynamics and single-spin flip methods (for details see ref. [15]). Standard text-book values for bulk iron as defined in OOMMF [16] package were used used in MM simulations ($A = 21 \times 10^{-12}$ J/m, $K = 48$ kJ/m^3, $M_s = 1.7 \times 10^6$ A/m).

In-plane SQUID magnetization measurements are performed between 10 K and 300 K (fig. 1) in the as-grown state (never exposed to magnetic field) or after demagnetization by cycling through minor loops. Since the domain wall width is comparable to the dot size, Fe dots with sub-100 nm diameters do not form multi-domain states[2]. For such dots, the coercivity and magnetic equilibrium state depend on the dot diameter (fig. 1): For diameters larger than ~ 60 nm, the coercivity is reduced, with a narrowing of the hysteresis loop close to the zero-magnetization states. For smaller diameters, the hysteresis loops resemble closely those of a random distribution of magnetic elements in single domain states. For simplicity, fig. 1 shows the comparison of two (out of many) hysteresis curves for 43 nm and 65 nm diameter dots. The ratio $\delta = W_{M=0}/W_{M=0.5M_s}$ of the hysteresis loop widths at $M = 0$ (zero magnetization) and $M = 0.5M_s$ (M_s: saturation magnetization) illustrates the effect of size on the hysteresis loop shape. Figure 2 shows the dependence of δ on the dot diameter obtained from both the experimental loops and MC simulations [15]. For dot diameters smaller than 60 nm, δ is ~ 1, corresponding to a single-domain spin configuration, as expected. For dot diameters close to 60 nm, this ratio is highly reduced due to the appearance of the narrowing ("neck") near zero magnetization.

This neck close to zero magnetization is attributed to the vortex state, as claimed earlier from MM simulation and MOKE [17]. In cylindrical ferromagnetic dots, microns or sub-micron in size, and with the diameter-to-thickness aspect ratio exceeding 1, the spin structure is mostly in-plane with a vortex-like curling spin arrangement that reduces the magnetostatic energy by flux closure. The topological singularity in the middle of the dot is resolved in the form of a vortex core —the region with an OOP magnetization. Switching from a single domain to the vortex state —the state with reduced magnetization— decreases the width of the hysteresis loop near zero magnetization.

In large diameter dots containing a vortex (*e.g.*, 1 μm Py dots), as the field is decreased from the high field saturated state, switching may occur into a vortex state in a positive field, resulting in zero remanent magnetization, and coercivity. In contrast, for smaller dots with reversal via vortex, the remanent state obtained after reducing the field to zero from the saturated state, is not a vortex state.

[2]The domain wall width, $\pi\sqrt{A/K}$, in Fe is estimated to be about 60 nm.

To overcome the energy barrier to form a vortex in small dots, several hundred Oersteds fields, applied opposite to the direction of saturation are required [15,18]. In the absence of a large enough reversal field, the system remains in a local minimum (the so-called "C-state" [15]) instead of going into the ground state vortex. The ground state at remanence can be observed in as-grown or demagnetized samples.

The energy barrier associated with vortex nucleation is consistent with the temperature dependence of the hysteresis curves. At $T = 300\,\mathrm{K}$, the neck is more pronounced than at $T = 10\,\mathrm{K}$, *i.e.* the coercive field and remanence are reduced at 300 K. This is consistent with the thermal activation of the switching to the vortex state, which leads to a less negative vortex nucleation field (when coming from positive saturation) [19]. Other contributions to the finite remanence and coercive field may include 1) small [14] inter-dot interactions, 2) contributions from very small single domain dots comprising the tail in the size distribution, and 3) deviations from smooth circular dots that tend to suppress vortex formation.

In addition to the narrowing of the hysteresis loops, the approach to saturation from the as-grown or demagnetized states is dramatically different for dots containing vortices. For dots (with diameters $< 60\,\mathrm{nm}$) in the single domain state, the initial ("virgin") magnetization curve is contained well inside the major hysteresis loop, while for larger dots ($> 60\,\mathrm{nm}$)— the virgin curve and the increasing branch of the hysteresis loops join at low fields [15]. Moreover, above 60 nm, below the vortex-annihilation field, the virgin curve is nearly linear and mostly reversible in a wide range of applied field ($M_r < 0.1 M_s$ for $H < 1\,\mathrm{kOe}$). This reversibility means that the vortex core returns to the center of the dot once the applied field is removed. As the applied field drives the vortex core across the dot boundary, the vortex is annihilated and the magnetization becomes irreversible[3]. MC [15] and MM [16] simulations reproduce the shape and reversibility of the virgin curve, provide vortex nucleation and annihilation fields close to experimental values and confirm that a vortex is the ground state.

Neutron scattering experiments. – To measure the OOP magnetization, M_z, of the vortex core and its diameter we perform polarized GI-SANS [20] with and without polarization analysis (at room temperature) for the dot sizes and field conditions which favor a vortex state. A $\sim 1.8\,\mathrm{cm}^2$ array of Fe dots with an average diameter $65 \pm 7\,\mathrm{nm}$, spacing $110 \pm 12\,\mathrm{nm}$ and thickness 20 nm is magnetically conditioned using the following protocol. First, a small, 34 Oe, field is applied perpendicular to the sample plane ($+\mathbf{z}$ in fig. 3(a)) to set the preferred direction for the vortex core magnetization (core polarity). Next, a second field of $-4\,\mathrm{kOe}$ is applied in the sample plane ($-\mathbf{y}$ in fig. 3(a)) to saturate the dots and then slowly increased to $+300\,\mathrm{Oe}$ – a field that exceeds the vortex nucleation field (fig. 1), before returning this field to zero, leaving only the 34 Oe along $+\mathbf{z}$ (see footnote [4]).

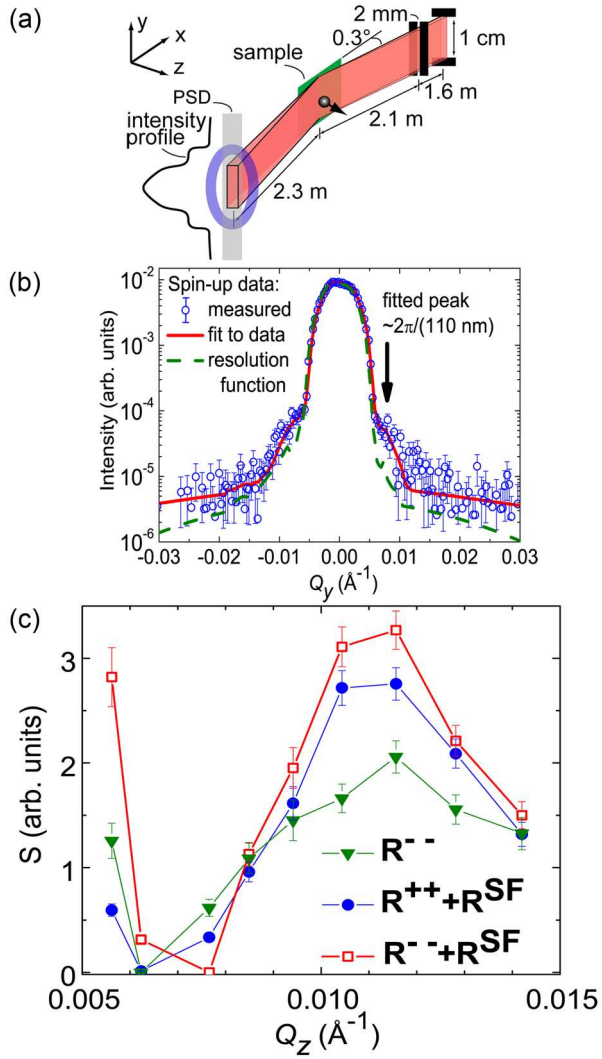

Fig. 3: (Colour on-line) (a) Schematic of the experimental setup. (b) Polarized neutron scattering as a function of scattering vector component Q_y for $Q_z = 0.011\,\mathrm{Å}^{-1}$. (c) Integrated neutron scattering intensity from the dots as a function of Q_z.

A portion of the intensity of neutrons scattered in a cone around the specularly reflected beam (fig. 3(a)) [21–23] is measured as a function of position and time of flight. This provides the Q_z and Q_y components of the wavevector transfer (the difference between the incoming and outgoing neutron wavevectors)[5].

Our experiment becomes most sensitive to the magnetization along the vortex core when the neutron beam

[3]The reversibility analysis is used with the First Order Reversal Curve FORC method to fingerprint the vortex state as described in ref. [18].

[4]The out-of-plane field is needed to maintain the polarization of the neutron beam and to set the direction of the vortex core magnetization, "vortex polarity".

[5]The vertical and horizontal divergences of incident neutron beam are 5 mrad and 0.6 mrad, respectively. The sample-to-detector distance is 2.35 m.

polarization (93%) is rotated along M_z, *i.e.* perpendicular to the sample surface. In this orientation the neutron scattering (non–spin-flip) differential cross-sections $\frac{d\sigma^{\pm\pm}}{d\Omega}$ depend on the neutron polarization (along ($^{++}$) or opposite ($^{--}$) to M_z). However, the in-plane magnetization causes some neutron beam polarization flip (since this magnetization is perpendicular to the neutron beam polarization axis) $\frac{d\sigma^{SF}}{d\Omega}$.

Neutron data are collected for Q_z from 0.005 to 0.15 Å^{-1} and Q_y in the range of ± 0.04 Å^{-1} for incident spin-up and spin-down polarization (without polarization analysis), yielding $\frac{d\sigma^{\pm\pm}}{d\Omega} + \frac{d\sigma^{SF}}{d\Omega}$. In addition, a third measurement for spin-down polarization with polarization analysis yielding only $\frac{d\sigma^{--}}{d\Omega}$ is made. The Q_y-dependence of $\frac{d\sigma^{++}}{d\Omega} + \frac{d\sigma^{SF}}{d\Omega}$ for $Q_z = 0.011$ Å^{-1} is shown ($\circ$) in fig. 3(b). Also shown in it is the neutron scattering measured from a continuous Co film also with OOP magnetization [24]. The excess intensity between the blue symbols and the green dashed curve is the small-angle scattering (diffraction) from the array of Fe dots.

Data analysis and results. – To extract the intensity of the small-angle scattering, we convolute a curve representing the small angle scattering (in the form of a Gaussian peak with integrated intensity S and centered at $\pm|Q_y^0|$), and the specular reflectivity (a delta function) with the instrumental broadening of the instrument (measured using the continuous Co film yielding the green dashed curve in fig. 3(b)). The optimum value of $|Q_y^0|$ yields a dot periodicity of 106 ± 9 nm, in agreement with the value obtained from the SEM images. The result for $Q_z = 0.011$ Å^{-1} is shown as the solid red curve in fig. 3(b) (there are nine such Q_y scans for different values of Q_z and for each of neutron spin-up, spin-down, and spin-down with polarization analysis). The intensities of the small angle scattering as a function of Q_z are shown in fig. 3(c). Integrating these values for $Q_z > 0.01$ Å^{-1}, where the neutron wave function is not purely imaginary (*i.e.* above the critical edge), gives (in arbitrary units)

$$\frac{d\Sigma^{++}}{d\Omega} + \frac{d\Sigma^{SF}}{d\Omega} = (8.9 \pm 0.3) \times 10^{-7},$$
$$\frac{d\Sigma^{--}}{d\Omega} + \frac{d\Sigma^{SF}}{d\Omega} = (10.1 \pm 0.3) \times 10^{-7},$$
$$\frac{d\Sigma^{--}}{d\Omega} = (8.8 \pm 0.3) \times 10^{-7}.$$

The spin asymmetry of the small-angle scattering defined as $P_a = \left(\frac{d\Sigma^{++}}{d\Omega} - \frac{d\Sigma^{--}}{d\Omega}\right) \Big/ \left(\frac{d\Sigma^{++}}{d\Omega} + \frac{d\Sigma^{--}}{d\Omega}\right) = -0.07 \pm 0.03$.

The non–spin-flip differential scattering cross-section $\frac{d\Sigma^{\pm\pm}}{d\Omega} = \tilde{C}\rho_{\pm}^2$ (see footnote [6]) is related to the appropriate spin-dependent scattering length density $\rho_{\pm}^2 = \rho_n^2 + \rho_{m_z}^2 \pm 2\rho_n\rho_{m_z}$, with ρ_n and ρ_{m_z} the nuclear and magnetic neutron scattering length densities, respectively. Hence,

$$P_a = 2\rho_n\rho_{m_z} \big/ \left(\rho_n^2 + \rho_{m_z}^2\right). \quad (1)$$

Solving this equation for ρ_{m_z} and using the literature value $\rho_n = 8 \times 10^{-6}$ Å^{-2} for Fe [20], we obtain the net OOP magnetization averaged over the volume of the dot, $m_z = 140 \pm 50$ emu/cm^3. This magnetization is equivalent to that of a 20 nm-thick Fe cylinder with a diameter of 19 ± 4 nm (which is found as 65 nm $\times \sqrt{m_z/M_s}$, using literature value of $M_s = 1714$ emu/cm^3), representing a vortex core (fig. 4(a)). The net OOP magnetization being opposite to the 34 Oe applied field ($P_a < 0$) confirms that it is not just a tilt of magnetization in response to that field.

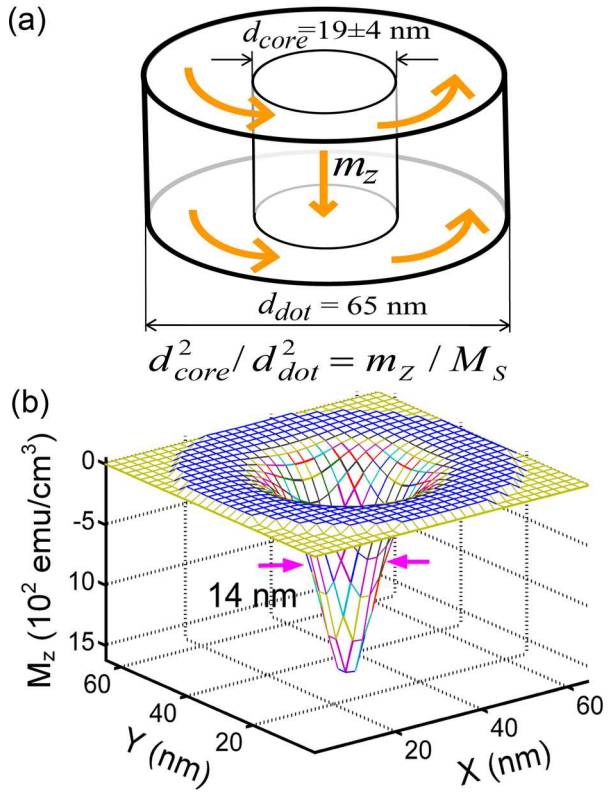

Fig. 4: (Colour on-line) (a) Sketch of magnetization in the 20 nm-thick Fe dot with the diameter of 65 nm (per neutron measurements). (b) Out-of-plane magnetization (M_z) profile of the vortex in the same dot, obtained using micromagnetic simulation.

Results of calculations. – The magnetization profile for a single 20 nm-thick Fe dot of 65 nm diameter obtained using MM simulation is presented in fig. 4(b). The corresponding $m_z = 78$ emu/cm^3 and the vortex core diameter, 14 nm, in qualitative agreement with the experimental result from neutron scattering. The difference is probably related to the fact that we used bulk parameters in the micromagnetic calculations. For instance, using $A = 42 \times 10^{-12}$ J/m instead of 21×10^{-12} J/m, results

[6] $\tilde{C}$ is a collection of spin-independent terms representing the density of dots, form and structure factors, etc. Its detailed derivation is to be published elsewhere.

in $m_z = 147\,\mathrm{emu/cm^3}$, and $d_{core} = 19\,\mathrm{nm}$, matching the experimental numbers extremely well. The corresponding values obtained using MC calculations are $103\,\mathrm{emu/cm^3}$ and $\sim 16\,\mathrm{nm}$. Simulations also show that the magnetic moments outside the vortex core are slightly canted, (*i.e.* have a small M_z component) opposite to the vortex core magnetization. Such canting has been previously observed in sub-micron dots [4]. The total magnetic moment of the canted magnetization outside of the core is $\sim 1.9 \times 10^{-15}\,\mathrm{emu}$, which is about 2.8 times smaller than the total magnetic moment of the core ($\sim 5.3 \times 10^{-15}\,\mathrm{emu}$). The OOP magnetization forms two concentric domains, thus reducing the magnetostatic energy by more than the added exchange energy. Similar concentric domains also appear in the analytical consideration [25] of a similar problem: circularly symmetric magnetization of an infinite thin film with OOP anisotropy. Specifically, zeros of $M_z(r)$ are found at the radii equal to $(3.1 + 5.8n)w$, where $n = 0$, 1, 2 ... is an integer, and w is a domain wall parameter $\sqrt{A/K}$ [25] (different from ours[7], as the anisotropy is different). The ratio of the radii of the zeros for $n = 0$ and $n = 1$ is $8.9/3.1 \approx 2.9$. For our MM simulations with the edge of the dot taken as the point corresponding to $n = 1$, this ratio is ~ 2.3, in fair agreement with the analytical result. Commensuration of these zeros [25] of $M_z(r)$ with the dot diameter may also be related to the variation of the vortex stability in the dots with different diameters, presented in fig. 2. The origin of the dependence of δ on the dot diameter requires further investigation.

Conclusions. – We have obtained evidence for the appearance of the magnetic vortex in 20 nm-thick Fe dots with diameters smaller than 100 nm, and a transition from the vortex state to a single domain with decreasing dot diameter and increasing applied field. Using polarized neutron scattering, we have measured the out-of-plane magnetization of the vortex core, $m_z = 140 \pm 50\,\mathrm{emu/cm^3}$ for 65 nm diameter dots, which implies a vortex core size of $19 \pm 4\,\mathrm{nm}$ in agreement with Monte Carlo and micromagnetic calculations.

* * *

We thank M. Viret and F. Ott for discussions and preliminary GI-SANS measurement. This work has benefited from the use of the Lujan Neutron Scattering Center (Asterix spectrometer) at LANSCE funded by US DOE-BES. We acknowledge support from US AFOSR and DOE (DMR-BES); Texas A&M University, Texas A&M University - CONACYT Collaborative Research Grant Program, FONDECYT (1050066, and 7070149), Millennium Science Nucleus (P06-022F); CONACYT (J-59853-F), KOSEF (R01-2008-000-21092-0), Spanish CYCIT (MAT2006-03999), Catalan Dursi (2005BE00028, 2005SGR00969), and U. Barcelona (International Cooperation).

[7] Domain wall width for Fe that was discussed earlier, see footnote [2].

REFERENCES

[1] Shinjo T., Okuno T., Hassdorf R., Shigeto K. and Ono T., *Science*, **289** (2000) 930.
[2] Miltat J. and Thiaville A., *Science*, **298** (2002) 555.
[3] Wachowiak A., Wiebe J., Bode M., Pietzsch O., Morgenstern M. and Wiesendanger R., *Science*, **298** (2002) 577.
[4] García-Martín J. M., Miltat J., Thiaville A., Okuno T., Vila L. and Piraux L., *J. Phys D: Appl. Phys.*, **37** (2004) 965.
[5] Li J. and Rau C., *Phys. Rev. Lett.*, **97** (2006) 107201.
[6] See *e.g.* Compton R. L. and Crowell P. A., *Phys. Rev. Lett.*, **97** (2006) 137202 and references therein.
[7] Buchanan K. S., Roy P. E., Grimsditch M., Fradin F. Y., Guslienko K. Y., Bader S. D. and Novosad V., *Nat. Phys.*, **1** (2005) 172.
[8] Chou K. W., Puzic A., Stoll H., Dolgos D., Schütz G., Van Waeyenberge B., Vansteenkiste A., Tyliszczak T., Woltersdorf G. and Back C. H., *Appl. Phys. Lett.*, **90** (2007) 202505.
[9] van Waeyenberge B., Puzic A., Stoll H., Chou K. W., Tyliszczak T., Hertel R., Fähnle M., Brückl H., Rott K., Reiss G., Neudecker I., Weiss D., Back C. H. and Schütz G., *Nature*, **444** (2006) 461.
[10] Choe S.-B., Acremann Y., Scholl A., Bauer A., Doran A., Stöhr J. and Padmore H. A., *Science*, **304** (2004) 420.
[11] Jung W., Castaño F. J. and Ross C. A., *Phys. Rev. Lett.*, **97** (2006) 247209.
[12] Villegas J. E., Li C.-P. and Schuller I. K., *Phys. Rev. Lett.*, **99** (2007) 227001.
[13] Li C.-P., Roshchin I. V., Batlle X., Viret M., Ott F. and Schuller I. K., *J. Appl. Phys.*, **100** (2006) 074318.
[14] Grimsditch M., Jaccard Y. and Schuller I. K., *Phys. Rev. B.*, **58** (1998) 11539.
[15] Mejía-López J., Altbir D., Romero A. H., Batlle X., Roshchin I. V., Li C.-P. and Schuller I. K., *J. Appl. Phys.*, **100** (2006) 104319.
[16] OOMMF code `http://math.nist.gov/oommf`.
[17] Prejbeano I.-L., Natali M., Buda L. D., Ebels U., Lebib A., Chen Y. and Ounadjela K., *J. Appl. Phys.*, **91** (2002) 7343.
[18] Dumas R. K., Li C.-P., Roshchin I. V., Schuller I. K. and Liu K., *Phys. Rev. B*, **75** (2007) 134405.
[19] Dumas R. K., Li C.-P., Roshchin I. V., Schuller I. K. and Liu K., *Appl. Phys. Lett.*, **91** (2007) 202501.
[20] Fitzsimmons M. R. and Majkrzak C. F., in *Modern Techniques for Characterizing Magnetic Materials*, edited by Zhu Y. (Kluwer, Boston) 2005, pp. 107–152.
[21] Wolff M., Scholz U., Hock H., Magerl A., Leiner V. and Zabel H., *Phys. Rev. Lett.*, **92** (2004) 255501.
[22] Wolff M., Magerl A. and Zabel H., *Eur. Phys. J. E*, **16** (2005) 141.
[23] Wolff M., Magerl A. and Zabel H., *Physica B*, **357** (2005) 84.
[24] Park S., Zhang X., Misra A., Thompson J. D., Fitzsimmons M. R., Lee S. and Falco C. M., *Appl. Phys. Lett.*, **86** (2004) 42504.
[25] Suhl H., *Relaxation Processes in Micromagnetics* (Oxford University Press, New York) 2007, pp. 176–184.